

# Soliton pair interaction law in parametrically driven Newtonian fluid

BY M. G. CLERC<sup>1,\*</sup>, S. COULIBALY<sup>2</sup>, N. MUJICA<sup>1</sup>, R. NAVARRO<sup>1</sup>  
AND T. SAUMA<sup>1</sup>

<sup>1</sup>*Departamento de Física, Facultad de Ciencias Físicas y Matemáticas,  
Universidad de Chile, Casilla 487-3, Santiago, Chile*

<sup>2</sup>*Laboratoire de Cristallographie et Physique Moléculaire (LACPM), UFR  
Sciences des Structures de la Matière et Technologies (UFR SSMT),  
Université de Cocody, Abidjan, Côte d'Ivoire*

An experimental and theoretical study of the motion and interaction of the localized excitations in a vertically driven small rectangular water container is reported. Close to the Faraday instability, the parametrically driven damped nonlinear Schrödinger equation models this system. This model allows one to characterize the pair interaction law between localized excitations. Experimentally we have a good agreement with the pair interaction law.

**Keywords:** dissipative soliton; pattern formation; particle-type solutions

## 1. Introduction

Pattern formation in out of equilibrium dynamical systems leads sometimes to the appearance of coherent or localized states, that is, a pattern extends over a limited space region and consists of only a few cells, eventually one, of the corresponding extended structure. During the last few years, emerging macroscopic particle-type solutions in dissipative systems have been observed in different fields, such as domains in magnetic materials, chiral bubbles in liquid crystals, current filaments in gas discharges, spots in chemical reactions, localized states in fluid surface waves, oscillons in granular media, isolated states in thermal convection, solitary waves in nonlinear optics, among other physical systems. In one-dimensional systems, localized states can be described as spatial trajectories that connect one steady state with itself, which means they are homoclinic orbits from the dynamical system point of view (see Couillet 2002 and references therein), while domain walls or interfaces are seen as spatial trajectories joining two different steady states—heteroclinic curves—of the corresponding spatial dynamical system (van Saarloos & Cross 1990). For quasi-reversible systems—time-reversible systems perturbed with small injection and dissipation of energy (Clerc *et al.* 1999*a,b*, 2000, 2001, 2008*a*)—the prototype model that exhibits

\*Author for correspondence ([marcel@dfi.uchile.cl](mailto:marcel@dfi.uchile.cl)).

One contribution of 14 to a Theme Issue ‘Topics on non-equilibrium statistical mechanics and nonlinear physics’.

localized structures or dissipative solitons is the parametrically driven damped nonlinear Schrödinger equation (Barashenkov & Zemlyanaya 1999). This model has been derived in several contexts to describe patterns and localized structures, such as vertically oscillating layers of water (Miles 1984; Zhang & Viñal 1995), nonlinear lattices (Denardo *et al.* 1992), optical fibres (Kutz *et al.* 1993), Kerr-type optical parametric oscillators (Longhi 1996), magnetization in an easy-plane ferromagnetic exposed to an oscillatory magnetic field (Barashenkov *et al.* 1991; Clerc *et al.* 2008*b*) and parametrically driven damped chain of pendula (Alexeeva *et al.* 2000). Interaction of dissipative solitons and boundary effects has been studied qualitatively—numerically and experimentally—in the framework of non-propagating hydrodynamic solitons (Wu *et al.* 1984; Wang & Wei 1997*a,b*). However, a quantitative study of the interaction of these particle-type solutions is absent to our knowledge.

The aim of this paper is to characterize theoretically and experimentally the interaction of the dissipative solitons in a vertically driven rectangular water container. Close to the Faraday instability, the parametrically driven damped nonlinear Schrödinger equation models this system. This model allows one to characterize the pair interaction law between localized states, which decreases exponentially with the distance between the dissipative solitons and is attractive or repulsive depending on whether they are in phase or out of phase, respectively. The merging of two attractive dissipative solitons is characterized by the radiation of two small perturbations and the appearance of only one dissipative soliton. Experimentally we have a good agreement with the pair interaction law.

## 2. Parametrically driven damped nonlinear Schrödinger equation

The dynamics of a layer of incompressible fluid that is driven by a sinusoidal force with frequency  $\Omega$  normal to the free surface is modelled by the dimensionless parametrically driven and damped nonlinear Schrödinger equation (Miles 1984; Zhang & Viñal 1995)

$$\partial_t \psi = -i\nu\psi - i|\psi|^2\psi - i\partial_{xx}\psi - \mu\psi - \gamma\bar{\psi}, \quad (2.1)$$

where  $\psi(x, t)$  is a one-dimensional complex field and  $\bar{\psi}$  stands for the complex conjugate of  $\psi$ . The surface displacement from flat interface  $h(x, t)$  and the velocity potential at the free surface  $\phi(x, t)$  are slave variables that are of the form  $h = \psi e^{-i\Omega t/2} + c.c.$  and  $\phi(x, t) = -i\psi e^{-i\Omega t/2} + c.c.$ , respectively (see Zhang & Viñal 1995 and references therein).  $\nu$  is the detuning parameter, which is proportional to the difference between the observed standing wave frequency and  $\Omega/2$ ,  $\mu$  is the damping parameter that is proportional to the kinematic viscosity of the fluid and  $\gamma$  is the forcing acceleration amplitude. For  $\mu = \gamma = \eta = 0$ , equation (2.1) becomes the well-known nonlinear Schrödinger equation (Newell 1985), which describes the envelope of an oscillatory system. This model is a time-reversal Hamiltonian system with the transformation  $\{t \rightarrow -t, \psi \rightarrow \bar{\psi}\}$ . The terms proportional to  $\mu$  and  $\gamma$  break the time-reversal symmetry, and represent energy dissipation and injection, respectively. The higher order terms in equation (2.1) are ruled out by a scaling analysis, since  $\mu \ll 1$ ,  $\nu \sim \mu \sim \gamma$ ,  $|\psi| \sim \mu^{1/2}$ ,  $\partial_x \sim \mu^{1/2}$  and  $\partial_t \sim \mu^{1/2}$ .

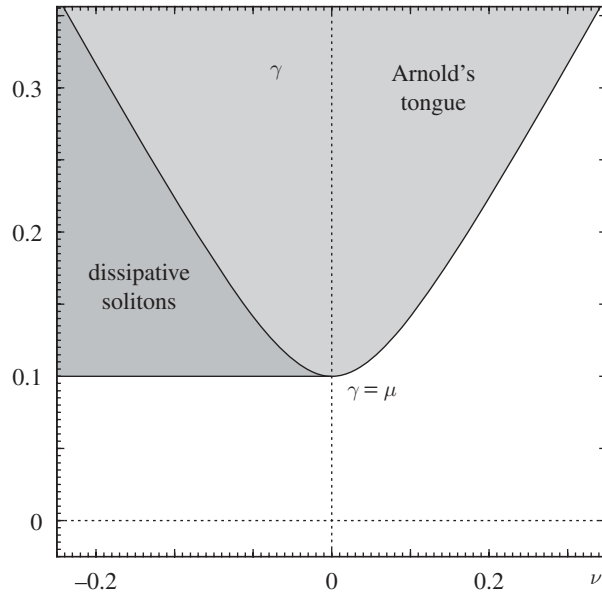


Figure 1. Bifurcation diagram of the parametrically driven damped nonlinear Schrödinger equation (2.1). The light grey area shows the Arnold tongue.

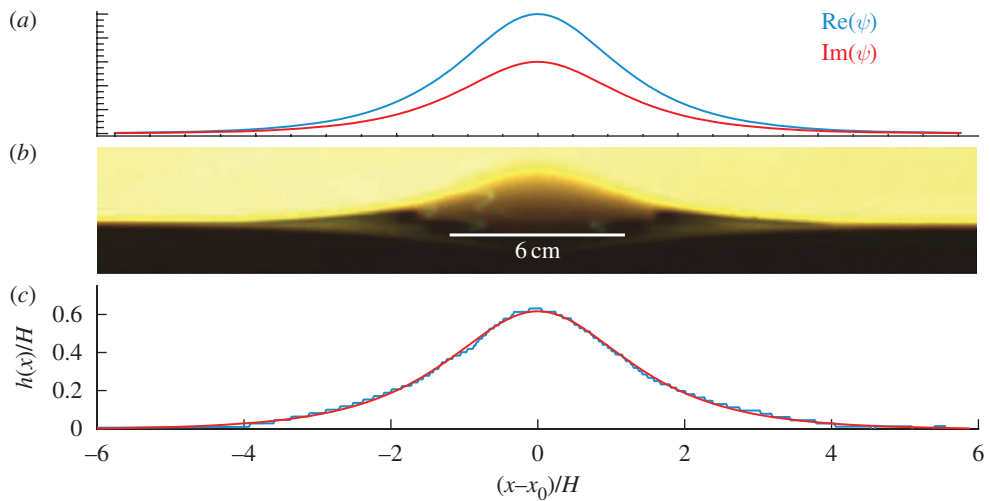


Figure 2. Dissipative soliton in parametrically resonant systems. (a) Stable dissipative soliton observed in the parametrically driven damped nonlinear Schrödinger equation model (2.1). (b) Snapshot of a non-propagating hydrodynamic soliton observed in a vertically driven 45 cm long and 2.54 cm wide rectangular container, filled with  $H = 1.5$  cm of water. Only two-thirds of the channel is shown. (c) Instantaneous surface profile (blue line) from image shown in (b). The solid red line shows the fit  $h(x) = A_s \operatorname{sech}[(x - x_0)/w]$ . Adjusted parameters are  $A_s/H = 0.63 \pm 0.02$  and  $w/H = 1.10 \pm 0.03$ .

A trivial state of equation (2.1) is the homogeneous state  $\psi_0 = 0$ , which represents the flat and quiescent solution of the fluid layer. For negative detuning,  $\nu < 0$ , the  $\psi_0 = 0$  state becomes unstable through a subcritical stationary instability at  $\gamma^2 = \mu^2 + \nu^2$  (cf. figure 1), which corresponds to a subharmonic instability of the flat fluid layer. Inside this region—the Arnold tongue—the system has three unstable uniform solutions  $\psi_0 = 0$ , and  $\psi_{\pm} = x_0 \pm i\sqrt{(\mu - \gamma)/(\mu + \gamma)}x_0$ , where  $x_0 \equiv \sqrt{(\gamma - \mu)(-\nu + \sqrt{\gamma^2 - \nu^2})/2\gamma}$ . These three states merge together through a pitchfork bifurcation at  $\gamma^2 = \mu^2 + \nu^2$ , with  $\nu > 0$ . However, for positive detuning, the quiescent state is only stable for  $\gamma < \mu$ , because this state exhibits a spatial instability at  $\gamma = \mu$ , which gives rise to a spatial periodic state with wave number  $k_c = \sqrt{\nu}$ . This state represents subharmonic surface waves—Faraday waves.

### (a) Dissipative solitons

For negative  $\nu$ , the parametrically driven damped nonlinear Schrödinger equation exhibits localized states supported asymptotically by the quiescent state. In order to obtain these localized states, we use the Madelung transformation  $\psi(x, t) = R(x, t)e^{i\theta(x, t)}$ , then the parametrically driven damped nonlinear Schrödinger equation reads

$$\partial_t R = 2\partial_x R \partial_x \theta + R \partial_{xx} \theta - \mu R + \gamma R \cos(2\theta), \quad (2.2)$$

$$R \partial_t \theta = -\nu R - R^3 - \partial_{xx} R + R(\partial_x \theta)^2 - \gamma R \sin(2\theta). \quad (2.3)$$

Non-trivial steady homoclinic solutions—solutions that connect the quiescent state with itself—of the previous model are (dissipative solitons; see Barashenkov *et al.* 1991 and references therein)

$$\cos(2\theta) = \frac{\mu}{\gamma}, \quad (2.4)$$

$$R_{\pm}(x) = \sqrt{2\delta_{\pm}} \operatorname{sech}\left(\sqrt{\delta_{\pm}}[x - x_0]\right), \quad (2.5)$$

where  $\delta_{\pm} \equiv -\nu \pm \sqrt{\gamma^2 - \mu^2} = -\nu - \gamma \sin(2\theta)$ . The amplitude and width of the dissipative solitons are characterized by  $\sqrt{2\delta_{\pm}}$  and  $1/\sqrt{\delta_{\pm}}$ , respectively. As a consequence of the spatial translation symmetry of model (2.1), the dissipative solitons are a family of states parametrized by a continuous parameter  $x_0$ . This parameter stands for the position of the maximum of the localized state. Figure 2a shows a typical dissipative soliton observed in the parametrically driven damped nonlinear Schrödinger equation. Hence, the above model has localized states if  $\nu < 0$ ,  $\gamma \geq \mu$  and  $\gamma^2 < \mu^2 + \nu^2$ . This parameter region is depicted by the dark grey area in figure 1. In this region, the relation  $\cos(2\theta) = \mu/\gamma$  has four solutions in the interval  $[-\pi, \pi]$ . Figure 3 illustrates this relation and the respective particle-type solutions. From this picture, one can infer that the localized states appear or disappear by simultaneous saddle-node bifurcations when  $|\gamma| = \mu$ . The support state of these localized states becomes unstable at the Arnold tongue, therefore the dissipative soliton becomes unstable at  $\gamma^2 = \mu^2 + \nu^2$  ( $\nu < 0$ ). The stable solutions are characterized by  $\operatorname{Re}(\psi)\operatorname{Im}(\psi) > 0$ , that is both fields are simultaneously positive or negative (Barashenkov *et al.* 1991). Hence, there are two types of stable dissipative solitons.

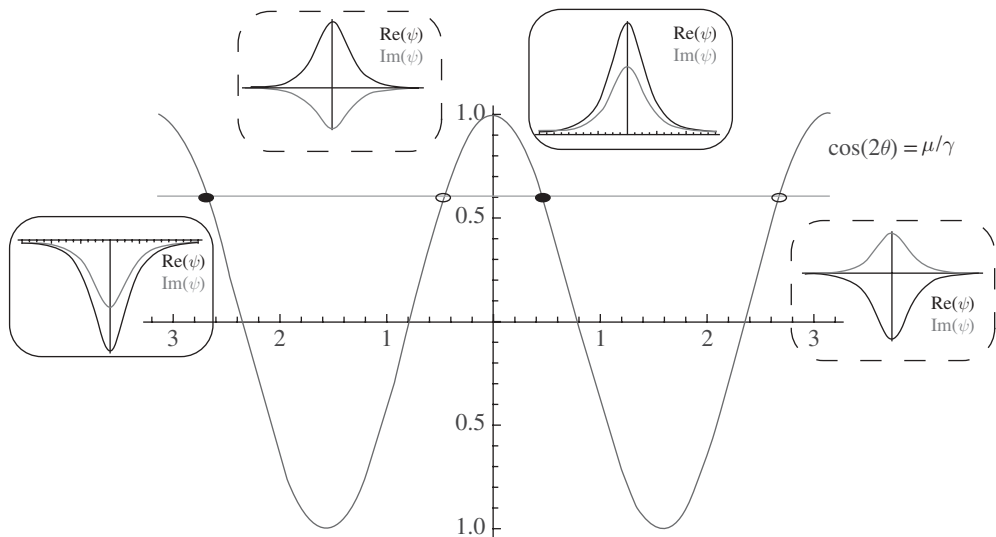


Figure 3. Schematic representation of the different dissipative solitons. The circles represent the different solutions of  $\cos(2\theta) = \mu/\gamma$ : filled (open) circles correspond to stable (unstable) localized states. The inset figures depict the different types of dissipative solitons.

In brief, close to the tip of the Arnold tongue, the dissipative solitons appear with finite amplitude by a saddle-node bifurcation at  $\gamma = \mu$ . Increasing the forcing amplitude  $\gamma$ , the amplitude and the width of stable dissipative solitons increase and decrease, respectively. Increasing  $\gamma$  more, these localized states become unstable at the Arnold tongue ( $\gamma^2 = \mu^2 + \nu^2$  and  $\nu < 0$ ). When one increases the modulus of the detuning—far from the tip of the Arnold tongue—the amplitude of the dissipative soliton exhibits an Andronov–Hopf bifurcation and increasing more the detuning the amplitude of the dissipative soliton exhibits double-period scenarios (Shchesnovich & Barashenkov 2002). Recently, these bifurcations have been verified experimentally (Zhang *et al.* 2007).

### 3. Derivation of pair interaction law

The interaction of dissipative solitons has been studied qualitatively—numerically and experimentally—in the framework of non-propagating hydrodynamic solitons (Wang & Wei 1997*a,b*). In particular, it has been shown that two dissipative solitons in a large channel that are in (out of) phase experience an attractive (repulsive) interaction. In order to study quantitatively this dynamical process, we consider two dissipative solitons that are initially well separated (remote pair of dissipative solitons), such that the distance between the respective maxima is larger than the typical soliton width. Figure 4 illustrates the configuration under study. In this circumstance, we can consider the ansatz

$$R(x, t) = R_+ \left( x + \frac{\Delta(t)}{2} \right) + \chi R_+ \left( x - \frac{\Delta(t)}{2} \right) + \rho(x, \Delta), \quad (3.1)$$

$$\theta(x, t) = \theta_0 + \varphi(x, \Delta), \quad (3.2)$$

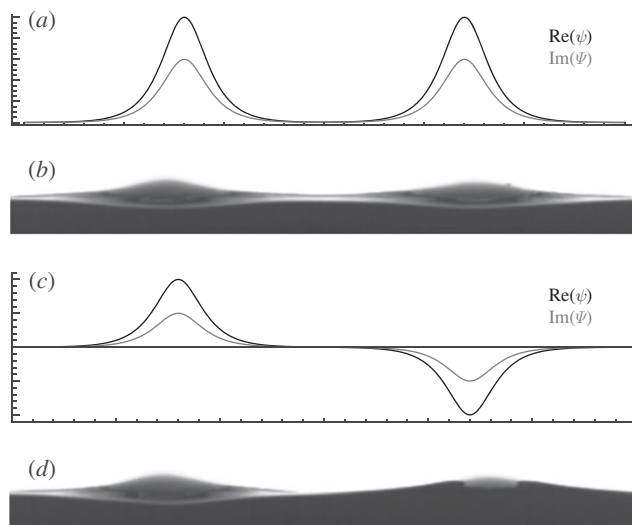


Figure 4. Dissipative soliton pair in parametrically resonant systems. (a) Two solitons in phase observed in model (2.1) and (b) in a vertically driven rectangular water container. (c) Two solitons out of phase observed in model (2.1) and (d) in a vertically driven rectangular water container.

where  $\Delta(t)$  accounts for the distance between the two maxima and  $\chi$  is a parameter that considers if dissipative solitons are in phase or out of phase, that is  $\chi = \pm 1$ . Hence, to take into account the effect of one localized state on the other one, we promote the soliton separation distance  $\Delta(t)$  to a variable—*parameter variation method*—and we modify slightly the dissipative soliton solutions including the small correction fields  $\rho(x, \Delta)$  and  $\varphi(x, \Delta)$  ( $\rho, \varphi \ll 1$ ). Furthermore, we consider  $\Delta \cdot \delta_+^{1/2} \gg 1$ . We can then assume that  $\Delta(t)$  evolves slowly in time ( $\ddot{\Delta} \ll \dot{\Delta} \ll 1$ ), since the effect of one dissipative soliton on the other one decreases exponentially with the distance between them (soliton tail). For simplicity, we introduce the notation

$$\begin{aligned} R_{+,+}(z_+) &= R_+(z_+ \equiv x + \Delta/2), \\ R_{+,-}(z_-) &= R_+(z_- \equiv x - \Delta/2), \\ W &= (R_{+,+} + \chi R_{+,-}), \end{aligned}$$

where  $z_+$  and  $z_-$  are the respective moving coordinates.

Introducing the above ansatz in equation (2.2) and linearizing in  $\rho$  and  $\varphi$ , we obtain

$$\frac{\dot{\Delta}}{2} (\partial_{z_+} R_{+,+} - \chi \partial_{z_-} R_{+,-}) = W \partial_{xx} \varphi + 2 \partial_x W \partial_x \varphi - 2 \sqrt{\gamma^2 - \mu^2} W \varphi. \quad (3.3)$$

This equation is integrable and we obtain the recursive relation

$$\varphi = \int_{-\infty}^x dx' \frac{\sqrt{\gamma^2 - \mu^2}}{W^2} \int_{-\infty}^{x'} dy W^2 \varphi(y, t) + \int_{-\infty}^x \frac{dx' \dot{\Delta}}{2 W^2} \int_{-\infty}^{x'} dy W (\partial_{z_+} R_{+,+} - \chi \partial_{z_-} R_{+,-}).$$

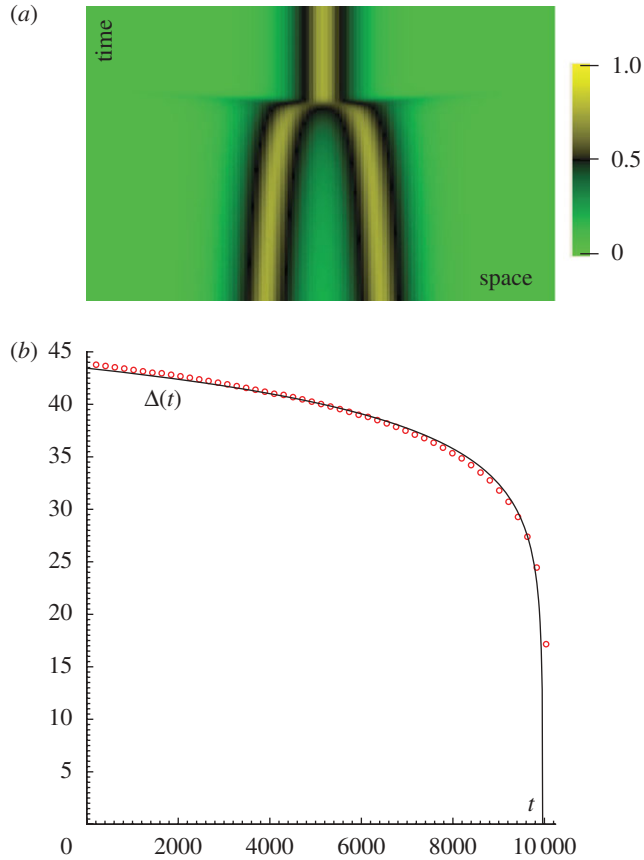


Figure 5. Interaction and collapse processes of two solitons. (a) Density plot of the spatio-temporal diagram of the imaginary part of  $\psi$  obtained by numerical simulation of model (2.1) with  $\mu = 0.115$ ,  $\gamma = 0.27$  and  $\nu = -0.063$ . (b) Temporal evolution of corresponding soliton distance  $\Delta(t)$ . Red circles stand for the soliton pair separation distance obtained numerically and the continuous curve is obtained from the formula (3.11).

Close to the saddle-node bifurcation ( $\gamma - \mu \ll 1$ ), we can use the Born approximation, that is,

$$\varphi = \dot{\Delta} \Theta(x, \Delta) + O(\sqrt{\gamma - \mu}), \tag{3.4}$$

with

$$\Theta(x, \Delta) \equiv \int_{-\infty}^x \frac{dx'}{2W^2} \int_{-\infty}^{x'} dy W(\partial_{z_+} R_{+,+} - \chi \partial_{z_-} R_{+,-}).$$

Hence, the phase correction is of the order of the temporal variation of distance between the dissipative solitons.

Analogously, we can introduce the ansatz (3.2) in equation (2.3) and linearizing in  $\rho$  and  $\varphi$ , we obtain

$$W \partial_t \varphi = \mathcal{L} \rho - 2\mu W \varphi - 3\chi R_{+,+}^2 R_{+,-} - 3R_{+,-} R_{+,+}^2 \tag{3.5}$$

with

$$\mathcal{L} \equiv -\nu + \sqrt{\gamma^2 - \mu^2} - 3(R_{+,+} + \chi R_{+,-})^2 - \partial_{xx}. \quad (3.6)$$

Using the approximation (3.4), the above equation reads at the dominant order

$$\mathcal{L}\rho = -2\mu W(x)\Theta(x)\dot{\Delta} - 3\chi R_{+,+}^2(x)R_{+,-}(x) - 3R_{+,-}(x)R_{+,+}^2(x). \quad (3.7)$$

Introducing the inner product

$$\langle f|g \rangle = \int_{-\infty}^{\infty} f(x)g(x) dx,$$

the linear operator  $\mathcal{L}$  is self-adjoint ( $\mathcal{L} = \mathcal{L}^\dagger$ ). The kernel of this linear operator—set of functions  $\{v\}$  that satisfy  $\mathcal{L}v = 0$ —is of dimension 2. Due to  $\mathcal{L}\partial_x R_{+, \pm} \approx 0$  being exponentially small ( $e^{-\delta_+^{1/2}\Delta}$ ), the functions  $R_{+, \pm}$  are pseudo-eigenfunctions of the kernel of  $\mathcal{L}$ . Therefore, the field  $\rho$  has a solution if (solvability condition)

$$\begin{aligned} &\langle \partial_{z+} R_{+,+} | 2\mu W\Theta \rangle \dot{\Delta} + \langle \partial_{z+} R_{+,+} | 3\chi R_{+,+}^2 R_{+,-} \rangle \\ &+ \langle \partial_{z+} R_{+,+} | 3R_{+,+} R_{+,-}^2 \rangle = 0. \end{aligned} \quad (3.8)$$

We obtain an equivalent result if we use the other element of the kernel  $\partial_{z+} R_{+,-}$  by  $\partial_{z+} R_{+,+}$ . Because  $\partial_{z+} R_{+,+}$  is a function of order one close to the soliton position of  $R_{+,+}$  and it decays exponentially close to the soliton position of  $R_{+,-}$ , then the last term of the above equation is neglected in comparison to the second one, that is

$$\dot{\Delta} = -\frac{3\chi \langle \partial_{z+} R_{+,+} | R_{+,+}^2 R_{+,-} \rangle}{2\mu \langle \partial_{z+} R_{+,+} | W\Theta \rangle}, \quad (3.9)$$

where

$$\langle \partial_{z+} R_{+,+} | W\Theta \rangle = \int_{-\infty}^{\infty} dz \partial_z R_{+,+} W(z) \int_{-\infty}^x \frac{dx'}{2W^2(x')} \int_{-\infty}^{x'} dy W(y) \Lambda(y)$$

is a positive number by symmetry arguments,  $\Lambda(y) \equiv \partial_{z+} R_{+,+}(y) - \chi \partial_{z-} R_{+,-}(y)$  and

$$\langle \partial_{z+} R_{+,+} | R_{+,+}^2 R_{+,-} \rangle = \int_{-\infty}^{\infty} dz \partial_z R_{+,+}(z) R_{+,+}^2(z) R_{+,-}(z + \Delta).$$

In order to estimate this integral, we evaluate it close to the soliton position of  $R_{+,+}$ , where  $R_{+,-}(z + \Delta) \approx \sqrt{2\delta_+} e^{-\delta_+(z+\Delta)}$  and then

$$\langle \partial_{z+} R_{+,+} | R_{+,+}^2 R_{+,-} \rangle \approx \sqrt{2\delta_+} e^{-\delta_+\Delta} \int_{-\infty}^{\infty} dz \partial_z R_{+,+}(z) R_{+,+}^2(z) e^{-\delta_+z}.$$

Hence,

$$\dot{\Delta} \approx -\mathcal{R}\chi e^{-\delta_+\Delta}, \quad (3.10)$$

where

$$\mathcal{R} = \frac{3\sqrt{2\delta_+} \int_{-\infty}^{\infty} dz \partial_z R_{+,+}(z) R_{+,+}^2(z) e^{-\delta_+z}}{\mu \int_{-\infty}^{\infty} dz \partial_z R_{+,+} W(z) \int_{-\infty}^x \frac{dx'}{2W^2(x')} \int_{-\infty}^{x'} dy W(y) \Lambda(y)}$$

is a positive constant. Therefore, the interaction between two dissipative solitons has an exponential law as function of the soliton distance. This interaction

is attractive (repulsive) when solitons are in (out of) phase, that is for  $\chi = 1$  ( $\chi = -1$ ).

For a given initial condition, we can integrate the evolution of the soliton distance and it takes the form

$$\Delta(t) = \delta_+^{-1} \ln[-\chi \delta_+ \mathcal{R}(t - t_0)], \quad (3.11)$$

where  $t_0$  is determined by the initial condition as

$$t_0 = \chi \frac{e^{\delta_+ \Delta(t=0)}}{\delta_+ \mathcal{R}}.$$

Hence, two dissipative solitons that are in phase are characterized by a logarithmic decrease of soliton separation distance. Figure 5 shows the temporal evolution of the soliton distance for two in-phase dissipative solitons. Red circles stand for the soliton pair separation distance obtained numerically and the continuous curve is obtained from the formula (3.11). Note that this formula has a quite good agreement even for small soliton distance, where this expression loses its soundness (cf. figure 5). In this case ( $\chi = 1$ ), the above expression is valid for  $t \leq \tau \equiv -1/\delta_+ \mathcal{R} + t_0$ , where  $\tau$  is the collapse time, the time for which both dissipative solitons merge together. Numerically, we observe that after the collapse, only one dissipative soliton survives. The process of two merging solitons is accompanied by the radiation of two perturbations as is depicted in figure 5a. A similar process is observed during the merging of two solitons in a non-integrable Hamiltonian system (Dyachenko *et al.* 1989). In this framework, to characterize the coarsening process was developed a statistical theory based on entropic arguments (Rumpf & Newell 2003). The interaction process described here does not render account of the collapse, and the subsequent radiation and prevalence of one dissipative soliton, because the validity of the pair interaction law is for remote dissipative solitons. Understanding this process and coarsening is in progress.

In the case of out-of-phase dissipative solitons ( $\chi = -1$ ), the pair interaction law is valid for  $t > t_0$ , where the parameter  $t_0$  is related to an initial time for which both dissipative solitons are close.

#### 4. Experimental study of the soliton pair interaction law

When a rectangular container partially filled with water is vertically driven at an appropriate frequency and amplitude, non-propagating hydrodynamic solitons can be observed (Wu *et al.* 1984; Wang & Wei 1997a,b). We have performed experiments in a vertically vibrating stainless steel channel with Plexiglas front and back walls,  $L_x = 45$  cm long,  $L_z = 9$  cm high, and  $L_y = 2.54$  cm wide. The channel is filled with water to a depth  $H = 1.5$  cm. Several drops of the wetting agent Kodak Photo-Flo are added to minimize surface pinning at the walls. The container is vibrated vertically with a harmonic oscillation of the form  $y(t) = A \sin(\omega t)$ , where the frequency under consideration is  $f = \omega/2\pi = 10.2$  Hz. Forcing is provided by means of a function generator (Agilent 33220A), whose sinusoidal signal is amplified by a power amplifier, which in turn feeds an electromechanical shaker (Dynamic Solutions VTS80). The amplitude  $A$  is the experimental control parameter that is of the order of

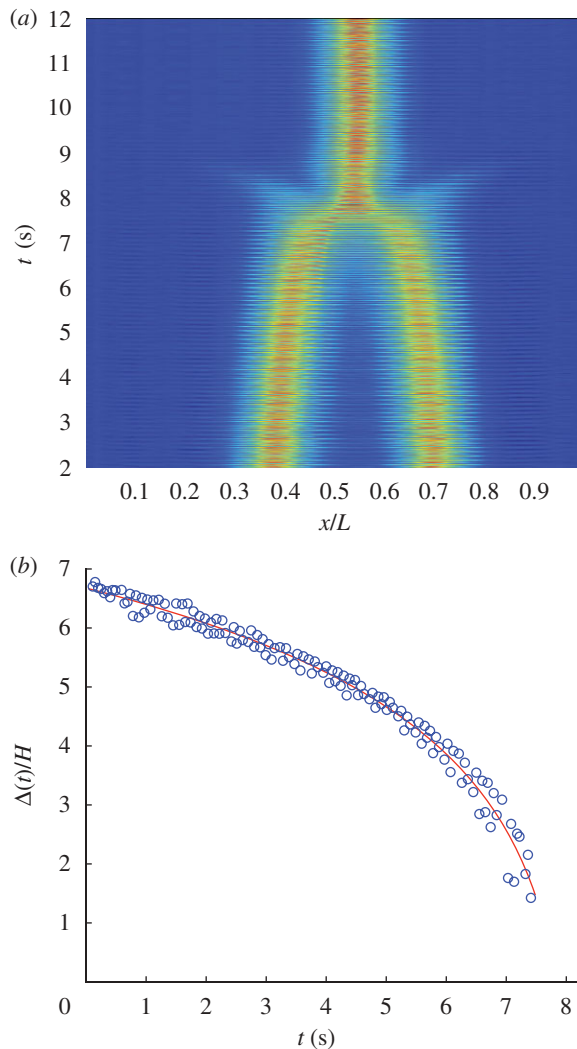


Figure 6. Interaction and collapse processes of two solitons in phase obtained experimentally in a vertically driven rectangular water container. (a) Density plot of the spatio-temporal diagram of the surface profile  $h(x, t)$ . (b) Temporal evolution of soliton separation distance  $\Delta(t)$ . Experimental data are shown with symbols (open circles) and the continuous curve is the corresponding fit  $\Delta(t) = a \cdot \ln(-b \cdot (t - t_0))$  motivated by formula (3.11). Adjusted parameters are  $a/H = 2.1 \pm 0.2$ ,  $b = 2.8 \pm 0.6 \text{ s}^{-1}$  and  $t_0 = 8.2 \pm 0.2 \text{ s}$ .

0.3 mm. Hence, the typical container acceleration is 10 per cent of the gravity acceleration. The container acceleration is measured by means of a piezoelectric accelerometer (PCB 340A65) connected to a lock-in amplifier (SR830) providing a precision of  $0.01\%g$ . Figure 2*b,c* show the characteristic non-propagating hydrodynamic soliton observed at a given time and the corresponding surface profile  $h(x)$ , where the soliton width and height are  $w = 1.65 \text{ cm}$  and  $A_s = 0.95 \text{ cm}$ , respectively.

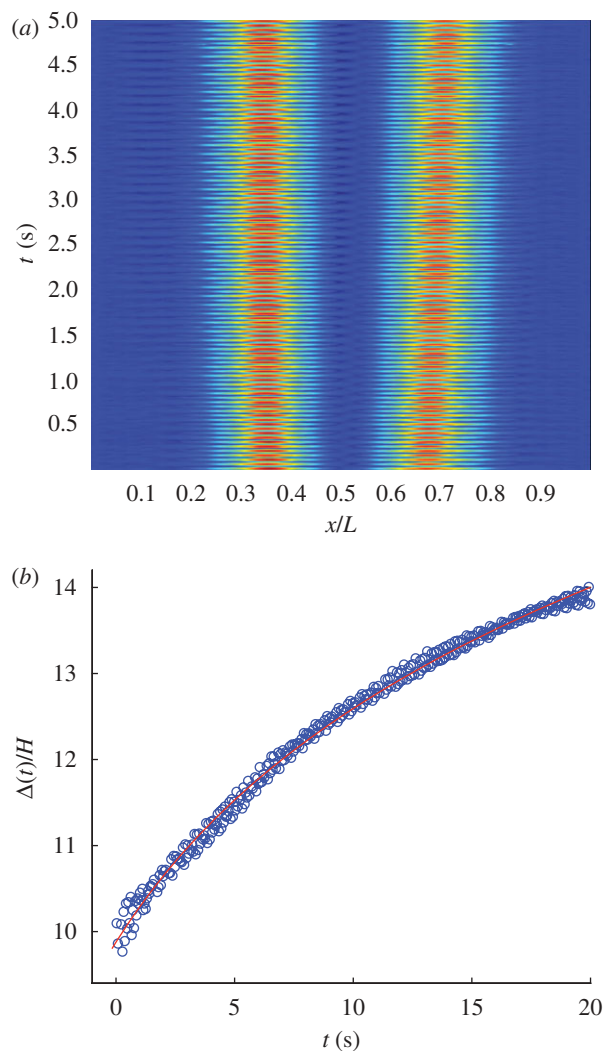


Figure 7. Interaction and collapse processes of two solitons out of phase obtained experimentally in a vertically driven rectangular water container. (a) Density plot of the spatio-temporal diagram of the surface profile  $h(x, t)$ . (b) Temporal evolution of soliton separation distance  $\Delta(t)$ . Experimental data are shown with symbols (open circles) and the continuous curve is the corresponding fit  $\Delta(t) = a \cdot \ln(b \cdot (t - t_0))$  motivated by formula (3.11). Adjusted parameters are  $a/H = 3.0 \pm 0.2$ ,  $b = 3.8 \pm 0.9 \text{ s}^{-1}$  and  $t_0 = 6.9 \pm 0.6 \text{ s}$ .

We have experimentally studied the interaction of two non-propagating hydrodynamic solitons. Close to the parametric resonance, this system is described by the parametrically driven damped nonlinear Schrödinger equation (Miles 1984; Zhang & Viñal 1995). Figure 4*b,d* depict snapshots of a pair of non-propagating hydrodynamic solitons in phase and out of phase, respectively.

These solitons are created manually with a metallic ruler, 2.5 cm wide, by ‘sloshing’ the water surface at a frequency close to the subharmonic response of the shaker (Wu *et al.* 1984). The relative phase of the two solitons is defined at

the creation of the second one, in principle randomly although the out-of-phase situation seems more easy to establish. In order to study their interactions, two solitons in phase are intended to be excited at a large separation distance but close enough such that their interaction dominates side-wall effects. Contrary, two solitons out of phase are intended to be excited close enough such that they are clearly distinct, but far enough such that the excitation of the second one does not destroy the first one. The cases reported here are representative cases of such good situations.

Figure 6*a* shows the spatio-temporal diagram of the surface profile  $h(x, t)$  obtained experimentally for two non-propagating hydrodynamic solitons in phase, which exhibit very similar dynamic behaviour to the one presented by the parametrically driven damped nonlinear Schrödinger equation. The temporal evolution of the separation distance  $\Delta(t)$  between the two non-propagating hydrodynamic solitons is presented in figure 6*b*. The continuous curve is the corresponding fit  $\Delta(t) = a \cdot \ln(-b \cdot (t - t_0))$  motivated by formula (3.11), which shows an excellent quantitative agreement with this model. The adjusted parameters are related to  $\delta_+$  and  $\mathcal{R}$ , which are then considered as free parameters in order to fit the experimental data. We note that in the experimental space–time diagram presented in figure 6*a*, we clearly observe two waves that are radiated from the two soliton collapse processes. As the final single soliton keeps the shape of an initial single stable soliton, the extra mass that is accumulated during the collapse of the two solitons has to be radiated towards the rest of the system.

An analogous analysis is performed with a pair of interacting non-propagating hydrodynamic solitons that are out of phase. A representative spatio-temporal diagram of the surface profile  $h(x, t)$  and the corresponding pair interaction law  $\Delta(t)$  is shown in figure 7. Again, an excellent agreement between the experimental data and the pair interaction law deduced in the theoretical framework of the parametrically driven damped nonlinear Schrödinger equation is obtained.

## 5. Conclusions

Conservative or time-reversible systems perturbed with small injection and dissipation of energy (quasi-reversal systems) can exhibit wealthy spatio-temporal dynamics. Parametrically driven quasi-reversal systems close to the parametric resonance are described in a unified way by the parametrically driven damped nonlinear Schrödinger equation. This model exhibits coherent states usually denominated dissipative solitons. These particle-type solutions are parametrized by one continuous parameter, the soliton position. We have deduced theoretically the pair interaction law for two remote localized states, which decreases exponentially with the separation distance and it is attractive (repulsive) for two dissipative solitons that are in phase (out of phase). Hence, we speculate that the dynamics of a dilute gas of dissipative solitons should be mediated by the pair interaction law. For example, we also expect that the coarsening dynamics of such dilute soliton gas should be dominated by the pair interaction law presented here. Work in this direction is in progress.

We have experimentally characterized the interaction law for two in-phase and out-of-phase non-propagating hydrodynamic solitons in a vertically driven rectangular water container. We have found a very good agreement with the pair interaction law deduced from the parametrically driven damped nonlinear Schrödinger equation. One of the main reasons for an exponential law for pair interaction is that the soliton tail affects the other non-propagating hydrodynamic soliton exponentially.

The authors thank Thomas Séon for his preliminary experimental study of non-propagating hydrodynamic solitons. The simulation software DimX developed at INLN, France, has been used for all the numerical simulations. We acknowledge the support of Anillo ACT 15 of the Programa Bicentenario de Ciencia y Tecnología of the Chilean government. M.G.C. and N.M. thank the support of FONDAPE grant 11980002. M.G.C., S.C. and N.M. thank the financial support of Fondecyt grants 1090045, 3080041 and 1070349, respectively.

## References

- Alexeeva, N. V., Barashennkov, I. B. & Tsironis, G. P. 2000 Impurity-induced stabilization of solitons in arrays of parametrically driven nonlinear oscillators. *Phys. Rev. Lett.* **84**, 3053–3056. (doi:10.1103/PhysRevLett.84.3053)
- Barashennkov, I. V., Bogdan, M. M. & Korobov, V. I. 1991 Stability diagram of the phase-locked solitons in the parametrically driven, damped nonlinear Schrödinger equation. *Europhys. Lett.* **15** 113–118. (doi:10.1209/0295-5075/15/2/001)
- Barashennkov, I. V. & Zemlyanaya, E. V. 1999 Stable complexes of parametrically driven, damped nonlinear Schrödinger solitons. *Phys. Rev. Lett.* **83**, 2568–2571. (doi:10.1103/PhysRevLett.83.2568)
- Clerc, M., Couillet, P. & Tirapegui, E. 1999a Lorenz bifurcation: instabilities in quasi-reversible systems. *Phys. Rev. Lett.* **83**, 3820–3823. (doi:10.1103/PhysRevLett.83.3820)
- Clerc, M., Couillet, P. & Tirapegui, E. 1999b The Maxwell–Bloch description of 1/1 resonances. *Opt. Commun.* **167** 159–164. (doi:10.1016/S0030-4018(99)00283-7)
- Clerc, M., Couillet, P. & Tirapegui, E. 2000 Reduced description of the confined quasi-reversible Ginzburg Landau equation. *Prog. Theor. Phys. Suppl.* **139**, 337–343.
- Clerc, M., Couillet, P. & Tirapegui, E. 2001 The stationary instability in quasi-reversible systems and the Lorenz pendulum. *Int. J. Bif. Chaos* **11**, 591–603. (doi:10.1142/S0218127401002316)
- Clerc, M. G., Encina, P. & Tirapegui, E. 2008a Shilnikov bifurcation: stationary quasi-reversal bifurcation. *Int. J. Bif. Chaos* **18**, 1905–1915. (doi:10.1142/S0218127408021440)
- Clerc, M. G., Coulibaly, S. & Laroze, D. 2008b Localized states beyond asymptotic parametrically driven amplitude equation. *Phys. Rev. E* **77**, 056 209. (doi:10.1103/PhysRevE.77.056209)
- Couillet, P. 2002 Localized patterns and fronts in nonequilibrium systems. *Int. J. Bif. Chaos* **12**, 2445–2457. (doi:10.1142/S021812740200614X)
- Denardo, B., Galvin, B., Greenfield, A., Larraza, A., Putterman, S. & Wright, W. 1992 Observations of localized structures in nonlinear lattices: domain walls and kinks. *Phys. Rev. Lett.* **68**, 1730–1733. (doi:10.1103/PhysRevLett.68.1730)
- Dyachenko, S., Zakharov, V. E., Pushkarev, A. N., Shvets, V. F. & Yankov, V. V. 1989 *Sov. Phys. JETP* **69**, 1144–1162.
- Kutz, J. N., Kath, W. L., Li, R. D. & Kumar, P. 1993 Long-distance pulse propagation in nonlinear optical fibers by using periodically spaced parametric amplifiers. *Opt. Lett.* **18**, 802. (doi:10.1364/OL.18.000802)
- Longhi, S. 1996 Stable multiple pulses in a nonlinear dispersive cavity with parametric gain. *Phys. Rev. E* **53**, 5520–5522. (doi:10.1103/PhysRevE.53.5520)
- Miles, J. W. 1984 Parametrically excited solitary waves. *J. Fluid Mech.* **148**, 451–460. (doi:10.1017/S0022112084002433)
- Newell, A. 1985 *Solitons in mathematics and physics*. Philadelphia, PA: Society for Industrial and Applied Mathematics.

- Rumpf, B. & Newell, A. C. 2003 Localization and coherence in nonintegrable systems. *Physica D* **184**, 162–191. (doi:10.1016/S0167-2789(03)00220-3)
- Shchesnovich, V. S. & Barashenkov, I. V. 2002 Soliton–radiation coupling in the parametrically driven, damped nonlinear Schrödinger equation. *Physica D* **164**, 83–109. (doi:10.1016/S0167-2789(02)00358-5)
- van Saarloos, W. & Hohenberg, P. C. 1990 Pulses and fronts in the complex Ginzburg–Landau equation near a subcritical bifurcation. *Phys. Rev. Lett.* **64**, 749–752. (doi:10.1103/PhysRevLett.64.749)
- Wang, X. & Wei, R. 1997*a* Dynamics of multisoliton interactions in parametrically resonant systems. *Phys. Rev. Lett.* **78**, 2744–2747. (doi:10.1103/PhysRevLett.78.2744)
- Wang, X. & Wei, R. 1997*b* Interactions and motions of double-solitons with opposite polarity in a parametrically driven system. *Phys. Lett. A* **227**, 55–60. (doi:10.1016/S0375-9601(97)00022-4)
- Wu, J., Keolian R. & Rudnick, I. 1984 Observation of a nonpropagating hydrodynamic soliton. *Phys. Rev. Lett.* **52**, 1421–1424. (doi:10.1103/PhysRevLett.52.1421)
- Zhang, W. & Viñal J. 1995 Secondary instabilities and spatiotemporal chaos in parametric surface waves. *Phys. Rev. Lett.* **74**, 690–693. (doi:10.1103/PhysRevLett.74.690)
- Zhang, L., Wang, X. & Tao, Z. 2007 Spatiotemporal bifurcations of a parametrically excited solitary wave. *Phys. Rev. E* **75**, 036602. (doi:10.1103/PhysRevE.75.036602)